Indonesian Journal of Chemical Research

http://ojs3.unpatti.ac.id/index.php/ijcr Indo. J. Chem. Res., 12 (2), 164-172, 2024

Synthesis And Characterization Of Silver Nanoparticles Using Gandaria (*Bouea macrophylla* Griff.) Seed Extract As Bioreductor And Ouw Natural Clay (ONC) As Matrix

Jaleha Kiat[1], Catherina M. Bijang[2*], Wayan Sutapa[2], Serly J. Sekewael[2]

[1]Inorganic Chemistry Laboratory, Mathematic and Natural Science Faculty, Pattimura University
[2]Chemistry Department, Mathematic and Natural Science Faculty, Pattimura University
[*]*Corresponding Author: rienabijang@yahoo.com*

Received: June 2024
Received in revised: August 2024
Accepted: September 2024
Available online: September 2024

Abstract

The synthesis of silver nanoparticles (AgNP) was achieved by utilizing gandaria seed extract as a bioreductant and Ouw natural clay (ONC) as a matrix. An investigation was conducted on the volume of a silver nitrate solution with a concentration of 1 x 10^{-3} M, which served as a precursor. The silver nanoparticles were analyzed using UV-Vis spectroscopy to assess their surface plasmon resonance (SPR) and stability. The results indicate that the SPR of silver nanoparticles occurs at a wavelength range of 432-450 nm. X-ray diffraction (XRD) was also employed for characterization purposes to ascertain the existence of silver nanoparticles that were generated within the ONC matrix. The XRD characterization data indicate that the Ag/ONC nanocomposite achieved the maximum stability and nanoparticle content when a volume of 500 mL of $AgNO_3$ 0.1 M (S5) was added. The mean crystal size of the silver nanoparticles generated is 48.48 nm, with a crystal orientation of both BCC (Body-Centered Cubic) and FCC (Face-Centered Cubic).

Keywords: Silver nanoparticles, Ouw Natural Clay, Gandaria seed extract, Bioreductor

INTRODUCTION

Nanotechnology refers to the scientific and engineering practices involved in the creation of materials, functional structures, and devices at the nanoscale scale. Nanometer-scale materials exhibit a range of chemical and physical properties that surpass those of macroscopic materials (bulk) (Abdullah & Khairurrijal, 2009). Nanotechnology plays a crucial role in advancing science and technology for the betterment of human life. Nanoparticles have undergone extensive investigation for several technological applications in the fields of materials science, chemistry, physics, biology, and environmental science (Wang et al., 2015; Sari et al., 2018). Nanotechnology plays a crucial role in advancing science and technology for the betterment of human life. Nanoparticles have undergone extensive investigation for several technological applications in the fields of materials science, chemistry, physics, biology, and environmental science (Sari et al., 2017). One of the materials synthesized as nanoparticles is silver (Jamaludin & Faizal, 2017; Fatimah & Aftrid, 2019; Irwan et al., 2023).

Indonesia rich in natural resources and having a diverse range of species, offers great potential for researching utilizing plants in the production of nanoparticles. Utilizing plant organic components in the manufacture of nanoparticles is a more environmentally conscious and streamlined approach (Rajan & Bhat, 2017). The underlying concept of biogenesis in nanoparticle manufacturing involves utilizing plants as reducing agents through the reduction process (Dubey et al., 2010; Handayani et al., 2014). Plant extracts containing secondary metabolite chemicals can be used to produce silver nanoparticles (AgNP) (Nyoman Wendri et al., 2017; Prasetiowati et al., 2018; Rahmayani et al., 2019). The gandaria plant (Bouea macrophylla G.) is a suitable bioreductor for AgNP production. The essential oil found in Gandaria fruit consists of hydrocarbons, terpenes, and oxygen-containing chemicals, including acids, alcohols, aldehydes, esters, and ketones (Bijang et al., 2023). Lolaen et al., (2013) conducted research that found that gandaria fruit juice contains phenolic compounds that have antioxidant properties. Meanwhile, (Londo et al., (2015) found that gandaria seed extract exhibits a

robust antioxidant activity that is nearly equivalent to that of vitamin C.

The manufacture of silver nanoparticles often leads to aggregation, resulting in the clustering of silver particles and their subsequent growth into larger particles, thus increasing their overall size (bulk). The stability of AgNP is crucial in its characterization and application to a product. To mitigate the formation of aggregates among nanoparticles, one can employ the strategy of introducing additional substances or applying a layer of molecules onto the particles (Salasa et al., 2016). Different kinds of clay, including zeolite and montmorillonite, have been employed as a medium for producing nanoparticles. Montmorillonite exhibits intercalation and ion exchange characteristics. The interlayer space of montmorillonite is suitable for synthesizing nanoparticle materials and biomaterials (Bijang et al., 2022).

Shameli et al., (2010) did research that demonstrates the ability to produce silver nanoparticles using chemical reduction procedures in the exterior space and interlayer of montmorillonite. The production of silver nanoparticles is directly influenced by the starting concentration of $AgNO_3$. The Maluku Province possesses a significant amount of untapped natural resources in the form of clay soil, which has not been fully utilized by the local population. The ONC discovered on Saparua Island primarily consists of Montmorillonite, a prevalent mineral (Bijang et al., 2021; 2022). This study employs natural resources from the Maluku province, specifically the gandaria plant as a bioreductor and natural Ouw clay as a matrix or anti-aggregation agent.

METHODOLOGY

Materials and Instruments

The tools was used consist of: a collection of glassware (Pyrex), a 100 mesh sieve, a Micro Pipette (Dragon LAB), a mortar and pestle, a spatula, an analytical balance (Ohaus), a hot plate (Cimerec 2), a magnetic stirrer, a vacuum pump (Vaccubrand), an oven (Shell Lab), a centrifuge (Biocen 22), a UV-Vis Spectrophotometer (Thermo), an FTIR instrument, and an XRD (Bruker D2 Phanser). The materials utilized in this experiment include ONC, Aquades, Deionized Water (WaterOne), H_2SO_4 (p.a Merck), $BaCl_2$ (p.a Merck), $AgNO_3$ (p.a Merck), Gandaria Seeds, Filter Paper, and Aquabides.

Methods

Preparation Method of ONC

ONC samples were collected and rinsed with distilled water, followed by drying in an oven at a temperature of 110° C for a duration of 2 hours. The dehydrated ONC was pulverized and filtered through a 100 mesh screen, yielding ONC powder.

The activation process involved the combination of 100 grams of ONC powder with 300 milliliters of 2 M H_2SO_4, while continuously stirring for 24 hours. The solution was subjected to filtration and rinsed with hot distilled water until it was completely devoid of sulfate ions (confirmed by testing with $BaCl_2$). Subsequently, it was dried in an oven at a temperature of 100°C. The dehydrated residue is placed into a desiccator and subsequently pulverized and filtered through a 100 mesh sieve.

Gandaria Seed Extract

The fifty grams of gandaria seeds are thoroughly washed, dried, and then cut into pieces before being ground using a blender. A quantity of 4.018 g of finely ground Gandaria seeds was measured and placed into an Erlemeyer flask. Subsequently, 400 mL of distilled water was added. Heat the mixture to a temperature of 100°C and agitate it with a magnetic stirrer until the extraction process is complete, indicated by a noticeable shift in color from purple to clear. Afterward filter the mixture. The water extract of gandaria seeds were labelled as EABG, was prepared at a concentration of 1% (w/v).

Synthesis of Ag/ONC Nanocomposites

Ag/ONC nanocomposites were synthesized by altering the silver content in the samples, namely at concentrations of 0.05%, 0.1%, 0.15%, 0.2%, and 0.5% Ag/10 g ONC. The 0.001 M $AgNO_3$ solution was prepared using several volumes: 0.05 L (S1), 0.1 L (S2), 0.15 L (S3), 0.2 L (S4), and 0.5 L (S5). 10 g of activated ONC was mixed with each litre of 0.001 M $AgNO_3$ solution and swirled for 24 hours at room temperature. A 25 mL solution of EABG with a concentration of 1% was added and agitated for 1 hour. The resulting mixture was then centrifuged at a speed of 3,000 revolutions per minute for a duration of 20 minutes. The solid material that formed as a result of the centrifugation was collected and then washed until all Ag^+ ions were removed. Finally, the washed material was dried at a temperature of 40°C.

Characterization of Ag/ONC Nanocomposites

UV-Vis spectrophotometry was used to measure the absorbance of ONC samples at a wavelength range of 320-500 nm. The measurements

were conducted both before and after the dispersion of Ag. Characterization was conducted with FTIR and XRD equipment. FTIR analysis is used to examine the absorption profile and any alterations that occur when produced with silver nanoparticles. FTIR measurements are conducted using the solid (powder) technique. The Ag/ONC nanocomposites were examined within the wavenumber range of 400-4000 cm-1. X-ray diffraction (XRD) analysis is employed to determine the crystal structure. The sample powder to be studied is weighed to around 0.5 g and then placed in the sample holder. The 2θ range of the sample is set to an angle of 5-85°. Once these adjustments are made, the sample can be analyzed using an X-ray diffractometer.

RESULTS AND DISCUSSION

Preparation of Ouw Natural Clay (ONC)

The clay utilized in this study is sourced from Saparua Island, specifically from Ouw Village. The ONC was rinsed with distilled water to eliminate contaminants and then subjected to drying at a temperature of 110°C. The drying process is conducted to eliminate residual moisture that remains confined within the interstitial spaces of the clay layers. The objective of ONC preparation is to purify and isolate ONC by removing contaminants such as sand, dirt, plant roots, and other associated components. During the preparation phase, the clay is passed through a 100 mesh sieve in order to standardize the particle size and enhance the surface area for ONC. The outcomes of our Natural Clay preparation are depicted in Figure 1.

Activation of ONC with Sulfuric Acid

The purpose of acid activation is to generate active sites on the surface and increase the interlayer spacing of clay. The activation procedure induces ion substitution and eliminates contaminants within the clay crystal structure, consequently enhancing the surface area and augmenting the clay's absorption capacity. In addition, the activation process is performed to achieve cationic equilibrium between the clay and the activating substance.

Figure 1. ONC preparation results

The utilized activation agent is sulfuric acid (H_2SO_4). Activation results in the substitution of cations in the clay interlayer, such as Ca^+, Na^+, and K^+, with H^+ cations derived from H_2SO_4. According to prior studies, the most effective concentration of H_2SO_4 for activating our natural clay is 2 M. The sieving procedure is performed to standardize the size and enhance the surface area of the clay, hence optimizing the interaction between the clay and the compounds utilized in the synthesis process. Rinsing the H_2SO_4-activated ONC with distilled water should be performed until the ONC is completely devoid of sulfate ions. The washing filtrate was treated with 5% solution of $BaCl_2$ to detect the presence of any leftover SO_4^- ions in activated ONC. This reaction resulted in the production of a white precipitate of BaSO4, which served as a characteristic identifier. The process of activating ONC results in a clay color that is brighter, namely a light brown shade, as compared to pure ONC. Figure 2 displays the outcomes of activated ONC.

Gandaria Seed Extraction

The Gandaria seed samples (Bouea macrophylla G.) underwent a process of cleaning and drying to eliminate contaminants and reduce surface water content. The gandaria seeds are fragmented and

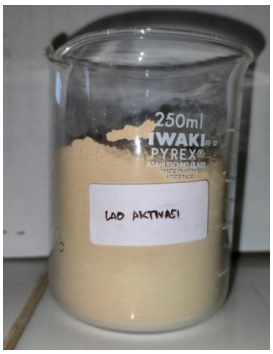

Figure 2. Activated ONC

pulverized with a blender to increase the contact area and facilitate the distribution of solvent in the extraction of gandaria seeds. The water extract of Gandaria seeds, referred to as EABG 1%, is prepared by dissolving 5.024 g of finely powdered Gandaria seeds in 500 mL of aquabides, which serve as the solvent.

The introduction of distilled water induces a transformation in the solution, resulting in a transparent purple hue. The color change seen is a consequence of the presence of anthocyanin, a pigment responsible for the purple color of Gandaria seeds. The extraction process was conducted at a temperature of 100°C for 1 hour. Subsequently, the solution was separated and passed through a filter. This continued until the solution transitioned from a distinct purple hue to a transparent state, while the Gandaria seed powder underwent a color transformation from purple to white. Subsequently, the solution of Gandaria seed extract was placed in an Erlemeyer jar, completely covering it, and secured with aluminum foil.

Synthesis of Ag/ONC Nanocomposites.

In this experiment, a 0.001 M solution of $AgNO_3$ was prepared using different volumes: 0.05 L (S1), 0.1 L (S2), 0.15 L (S3), 0.2 L (S4), and 0.5 L (S5). Subsequently, activated ONC was added, resulting in the formation of a brownish solution. The combination underwent a reaction by continuous stirring for 24 hours, during which a noticeable change in color from yellow to brown occurred. Subsequently, a water extract derived from Gandaria seeds was introduced into the mixture and swirled for a period of 1 hour. The suspension underwent centrifugation at a speed of 3,000 rpm for a duration of 20 minutes. The resulting precipitate was then collected and subjected to multiple washes until it was completely devoid of Ag^+ ions. Subsequently, the precipitate was dried at a temperature of 40°C. Finally, the maximum wavelength was determined using a UV-Vis spectrophotometer.

UV-Vis Spectrophotometric Characterization

Silver nanoparticles develop, leading to an augmentation in Surface Plasmon Resonance (SPR). The dependence of Surface Plasmon Resonance

Figure 3. Gandaria Seed Extract

(SPR) on the size, shape, and dielectric characteristics of the particle and its surroundings results in distinct SPR ranges for each particle type. Typically, the color shift happens as a result of the reduction of silver ions using the bioreductor found in EABG. Nevertheless, this alteration in color cannot serve as the primary signal of nanoparticle production. Tests must be conducted to verify the creation of nanoparticles, with one method being the utilization of UV-Vis spectrophotometry. UV-Vis spectrophotometry is used to examine the absorbance and optimal wavelength of silver nanocomposites. Additionally, it is employed to study the surface plasmon resonance (SPR) in silver nanoparticle colloids. Surface Plasmon Resonance (SPR) is a phenomenon in which the mobility of electron clouds in nanocomposite colloids is affected by the presence of radiation, resulting in oscillation and resonance. Silver nanoparticles agglomerate, the surface plasmon resonance (SPR) of the particles shifts to a longer wavelength. This shift occurs because the optical properties of the silver nanoparticles change, causing the conduction electrons near the particle's surface to become delocalized and shared with other particles. As a result, the SPR moves to a lower energy state, causing the absorption peak to shift to a longer wavelength.

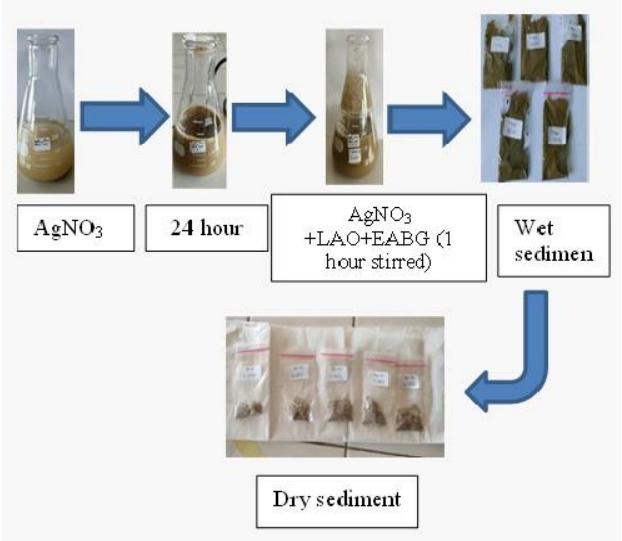

Figure 4. Synthesis of Ag/ONC nanocomposites.

Shameli et al., (2010) conducted a previous study that demonstrated the successful production of silver nanoparticles in a Montmorillonite (MMT) matrix through qualitative analysis using UV-Vis tests. The research findings indicated the occurrence of Surface Plasmon Resonance (SPR) within the wavelength range of 398-402 nm. This observation served as an early benchmark to validate the presence of silver nanoparticles in the ONC matrix. The measurement results indicate that the surface plasmon resonance (SPR) of Ag/ONC nanocomposites occurs at around 430-450 nm, and the absorbance intensity

shows a rise from S1 to S5 (Figure 5). The UV-Vis S1 measurements on day 0 indicated the presence of surface plasmon resonance (SPR) at a wavelength of 432 nm. On day 1, the SPR was still observed at the same wavelength, but the absorbance dropped. On the second day, it exhibited SPR (Surface Plasmon Resonance) in the wavelength region of 431-441 nm, reaching its highest level of absorption. Sample S2 exhibited surface plasmon resonance (SPR) at a wavelength of 433 nm on both day 0 and day 1. However, the absorbance on day 1 decreased compared to day 0. On the second day, the surface plasmon resonance (SPR) occurred at wavelengths between 430 and 449 nm, reaching its highest level of absorption. On day 0, the sample S3 exhibited a surface plasmon resonance (SPR) at a wavelength of 432 nm. On day 1, the SPR shifted to a wavelength of 433 nm, accompanied by a decrease in absorbance. On the second day, S3 exhibited surface plasmon resonance (SPR) in the wavelength region of 431-443 nm, with the highest level of absorption. Sample S4 exhibited consistent surface plasmon resonance (SPR) at a wavelength of 432 nm on both days 0 and 1. However, on day 2, the SPR was observed within the range of 430-450 nm. During day 0, the sample S5 exhibited surface plasmon resonance (SPR) at a wavelength range of 432 - 433 nm. On day 1, the SPR of the sample was seen at a wavelength of 432 nm, with the highest level of absorbance. On the second day, the surface plasmon resonance (SPR) occurred at a wavelength range of 430-450 nm, exhibiting the highest level of absorption. In this study, the Ag/ONC nanoparticle sample S5 is deemed to be the most stable due to its longer SPR wavelength range.

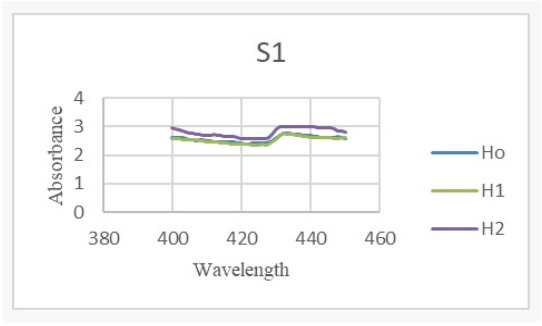

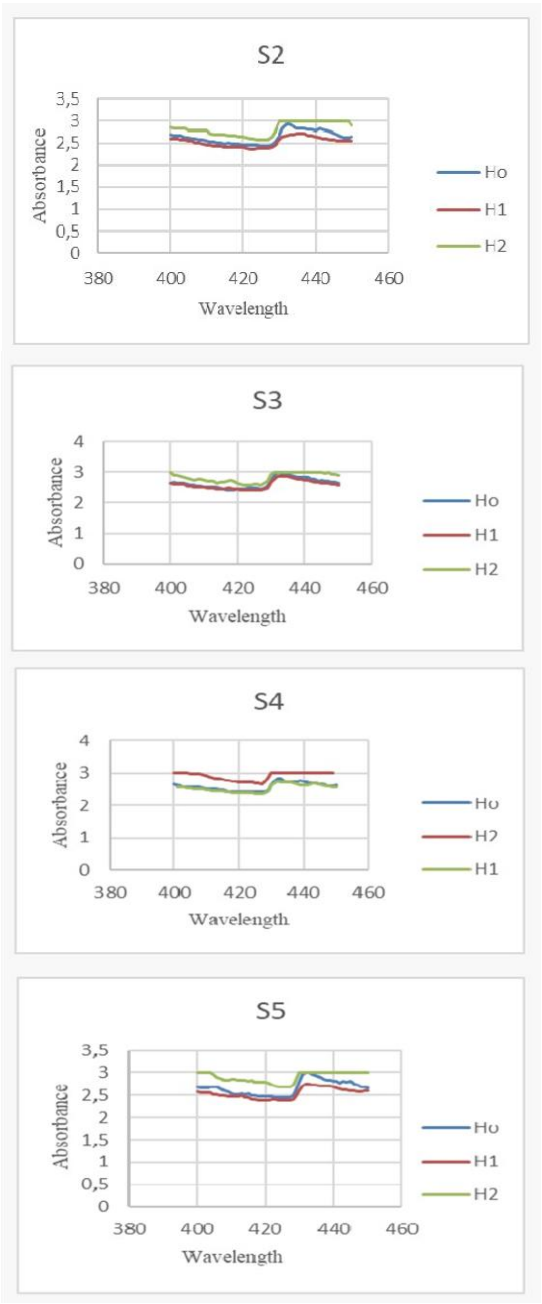

Figure 5. UV-Vis Results of S1-S5

FTIR Characterization

A strong absorption band with a wave number of 1029 cm-1 suggests the existence of -SiO and -AlO groups, which are distinctive features of the montmorillonite structure. The absorption bands seen at wavelengths 3622, 3446, 1633, 1029, 914, 794, 532, and 468 cm^{-1} indicate the properties of ONC, as indicated by prior studies (Figure 6).

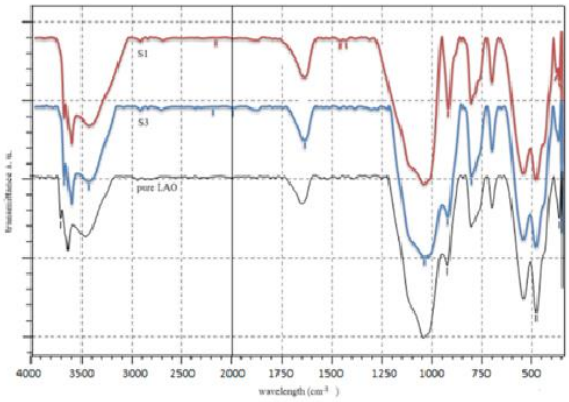

Figure 6: FTIR Characterization Results

Furthermore, these findings elucidate that the constituent mineral of ONC is a montmorillonite, a specific sort of mineral. The analysis of the montmorilonite infrared spectrum is presented in Table 1. According to the information in Table 1, the FTIR spectrum exhibits an absorption at 3697 cm^{-1}, indicating stretching vibrations of -OH. Additionally, there is a presence of stretching vibrations of -OH in water molecules situated in the clay interlayer, observed at 3446 cm^{-1}. The absorption at 1029 cm^{-1} is a characteristic of Si-O-Si or SiO_2 (quartz). The absorption at 794 cm^{-1} corresponds to Al-OH, while the absorption at 914 cm^{-1} represents the OH bending vibration of Al_2OH and Mg-OH. Lastly, the bending vibrations of Si-O occur at 527 cm^{-1} and 446 cm^{-1}.

The wave number shift seen in the IR spectra of S1 is not substantial when compared to the results of S3 synthesis with ONC, as depicted in Figure 8. The shift observed at wave numbers in the 3400 cm^{-1} range corresponds to the vibration of the -OH group in water molecules. This shift is believed to be caused by the replacement of H^+ ions with Ag^+ ions in the interlayer space, which disrupts the structure of the clay. As a result, the intensity of the -OH absorption peak decreases and a shift towards a lower wave number, specifically 3446 cm^{-1}, occurs. The specific wave numbers are 3442 cm^{-1} (S1), 3446 cm^{-1} (S3), and 3446 cm^{-1} (ONC). There is a change in the wave number seen in the absorption area of 1400 cm^{-1}. In pure natural clay, the wave number is 1406 cm^{-1}, while in activated natural clay it is 1436 cm^{-1}. However, in Ag/ONC nanocomposites, the wave numbers are 1427 cm^{-1} (S1), 1458 cm^{-1} (S3), and 1458 cm^{-1} (ONC). The results validate that the presence of a greater quantity of Ag nanoparticles leads to the emergence of van der Waals contacts between the oxygen groups in the clay and the Ag nanoparticles.

Table 1. Analysis Montmorillonite Infra Red Spektrum

Wave Number (cm^{-1})				
Pure ONC	SA	SB	SC	Functional Group Absorption
3622	3622	3697	3622	O-H stretching vibration
3446	3442	3446	3446	O-H stretching vibration of water molecules
1633	1637	1637	1643	H_2O bending vibrations of water molecules
1029	1033	1031	1031	Si-O asymmetric stretching vibration
914	912	914	914	O-H bending vibration of Al-OH
794	796	794	794	Symmetric stretching vibration of Si-O and Al-O
532	534	534	534	Al-O bending vibration
468	470	470	470	Si-O bending vibration

The presence of the peak at 2912.51 cm^{-1} in the FTIR analysis indicates the occurrence of stretching vibrations of -C-H (aldehyde) bonds. The FTIR analysis of the resultant AGNP product reveals the presence of a -OH group, which is involved in the reduction process. The results suggest that the phenolic compounds present in gandaria seeds have the ability to bind Ag^+ ions and convert them to Ag^0 on the surface of nanoparticles. This binding process

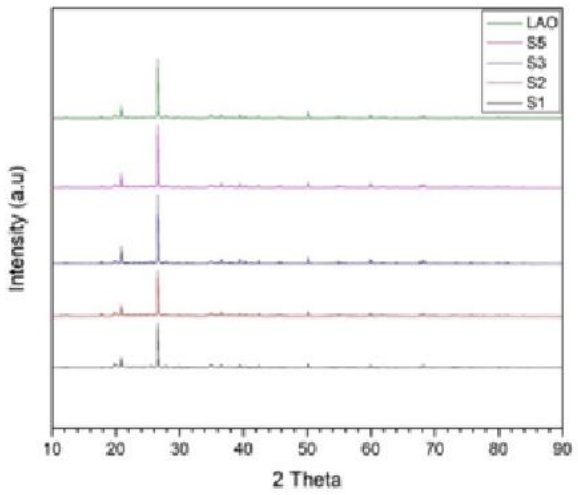

Figure 8. Diffractograms of ONC and Ag/ONC nanocomposites

is facilitated by the presence of free hydroxy groups, which act as capping agents and help stabilize the AgNP. During the reduction process, an electron donor is involved, causing the Ag^+ ion to be reduced to Ag^0.

The electron donor can originate from hydroxide ions or double bonds. Furthermore, there were absorption peaks seen at wave numbers 1456.26, 1427.32, 1379.10, and 1307.74 (S1), 1468.18, 1384.89, 1300.02, and 1269.16 (S3), and 1458.18, 1384.89, and 1301.95 cm^{-1} (ONC). These peaks correspond to the region of aromatic C=C absorption. Peaks 1033.85 (S1), 1031.92 (S3), and 1031.92 cm^{-1} (ONC) were identified as –C–OR and –O–H bonds with high intensity.

IV.5.3. XRD Characterization

X-ray diffraction (XRD) analysis was conducted to characterize the silver nanoparticles and determine their specific properties after synthesis. The diffractogram of Ag has a peak at the diffraction angle (2ɵ) as documented in the Joint Committee on Powder Diffraction Standards (JCPDS) data. The standard diffraction data for Ag are 39.53, 44.07, 64.44, 77.55, and 81.31 (Figure 7). Figure 7 reveals that the Miller index for each diffraction peak is {111}, {200}, {220}, {311}, and {222}. The diffractogram results of the Ag/ONC nanocomposite (Figure 8) show that there is a match with the normal Ag diffraction data, namely at peaks with intensities of 39.53, 44.07, and 64.43. The peak with the greatest intensity is denoted as S5. The peak seen at an angle of 2θ = 62.10° corresponds specifically to montmorillonite (PRD Ref.No.00-003-0010). The strength of this peak diminishes as the amount of AgNP in the montmorillonite matrix increases. Sample S5 exhibited the lowest intensity. This suggests that the sample contains the greatest quantity of AgNPs. Figure 8 illustrates that the ONC peaks remain unchanged compared to the diffraction pattern of Ag/ONC. This suggests that the Ag/ONC composite is formed through physical interactions.

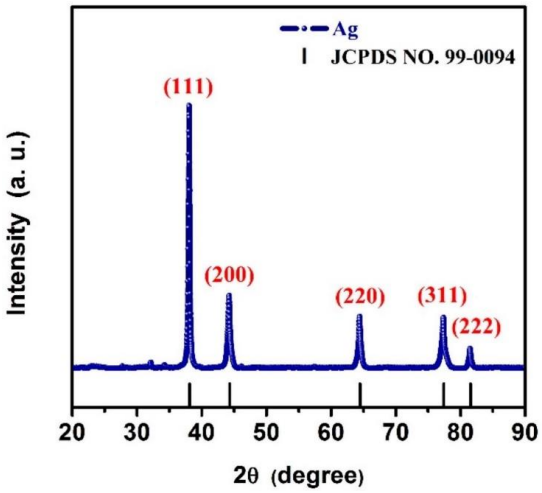

Figure 7. Standard diffractogram of silver nanoparticles

The XRD study in Figure 8 reveals the interplanar distances of the silver nanoparticles to be 0.227 nm (39.53º), 0.206 nm (44.07º), and 0.144 nm (64.43º). The Debye-Scherrer formula can be used to determine the average crystal size of silver nanoparticles by referring to the 2θ angle.

$$D = \frac{k\ x\ 0{,}1541\ nm}{\beta\ \mathrm{x}\cos\theta} \text{.....(1)}$$

The variables in the equation are defined as follows: D represents the average size of silver nanoparticle crystals, k is the Debye-Scherrer constant, β is the Full Width at Half Maximum (FWHM) of each peak, 0.1541 nm represents the wavelength of the X-ray radiation source, and θ represents the diffraction angle.

The results of calculations using equation 1 show that the average crystal size of the silver nanoparticles produced is 48.48 nm. Meanwhile, the results of calculating the lattice parameters of the silver nanoparticles produced in Table 1 show an average lattice parameter of 0.43 nm. The lattice parameters obtained are close to the lattice parameter

values of silver nanoparticles based on JCPDS no. 04-0783 (a=0.407 nm).

Table 2. Diameter sizes and lattice parameters of silver nanoparticles

2θ (º)	FWHM (º)	hkl	D (nm)	d-spacing (nm)	lattice parameters (a) nm
39,53	0,155	111	48,44	0,227	0,39
44,06	0,181	200	40,86	0,206	0,41
64,42	0,197	220	34,29	0,144	0,48
77,55	0.285	311	21,84	0,123	0,43
	Average		**48,48**	**0,175**	**0,43**

The crystal's propensity to adopt a specific plane orientation can be ascertained by determining the structure's orientation. The crystallographic orientation of a polycrystalline sample provides information about the degree of uniformity in the arrangement of crystals within the sample, as well as any variations in the electrical characteristics of the sample (Jenkins, 2006). The crystal orientation findings obtained from the X-ray diffraction (XRD) test are presented in Table 2, indicating the predicted crystal form for each peak. According to JCPDS data, silver exhibits two crystal orientations, specifically FCC (face-centered cubic) and BCC (body-centered cubic). Table 3 indicates that the peak observed at an angle of 2θ: 39.53º suggests a preference for the FCC crystal orientation. The FCC (Face-Centered Cubic) structure of silver entails the presence of silver atoms at each corner. In addition, there will be atoms located on every face of the cube.

Table 3. Structure orientation analysis of silver nanoparticles

No	2θ	h k l	S ($h^2+k^2+l^2$)	Crystal orientation
1	39.53	1 1 1	3	FCC
2	44.06	2 0 0	4	BCC, FCC
3	64,42	2 2 0	10	BCC

Peaks exhibiting an angle of 2θ: 44.06º are commonly associated with body-centered cubic (BCC) and face-centered cubic (FCC) orientations. This circumstance suggests that the crystals present at this peak may represent a transition between the face-centered cubic (FCC) and body-centered cubic (BCC) crystal structures. The peak observed at an angle of 2θ: 64.42º is expected to correspond to a body-centered cubic (BCC) crystal orientation. The BCC crystal orientation consists of 8 atoms located at each corner of the cubic unit cell, as well as one atom positioned at the middle of the cube.

CONCLUSION

The bioreduction of silver nanoparticles can be achieved by utilizing gandaria seed extract, as evidenced by the observable color change and the emergence of the surface plasmon resonance (SPR) peak in the UV-Vis spectrum. The UV-Vis analysis reveals that the silver nanoparticles, synthesized using the Gandaria seed extract as a bioreductant, exhibit a surface plasmon resonance (SPR) at a wavelength of 432-450 nm. The XRD analysis demonstrates that the Ag/ONC nanocomposite, obtained by adding 500 mL of 0.1 M $AgNO_3$ (S5), exhibits high stability and a significant nanoparticle content. The silver nanoparticles have an average crystal size of 48.48 nm, and their crystal orientation is a combination of body-centered cubic (BCC) and face-centered cubic (FCC) structures.

Acknowledgement

This work has been funded by Directorate General of Higher Education at the Indonesia Ministry of Education, Culture, Research, and Technology under the programme of Basic Excellence Research Grants for Higher Education 2024.

REFERENCES

Abdullah, M., & Khairurrijal. (2009). Karakterisasi Nanomaterial. *Jurnal Nanosains & Nanoteknologi*, *2*(2), 1–9.

Bijang, C. M., Tanasale, M. F. J. D. P., Kelrey, A. G., Mansur, I. U., & Azis, T. (2021). Preparation of Natural Ouw Clay-Chitosan Composite and Its Application as Lead and Cadmium Metal Adsorbent. *Indonesian Journal of Chemical Research*, *9*(1), 15–20.

Bijang, C.M., Nurdin, M., Latupeirissa, J., Aziz, T., & Talapessy, F. (2022). The Ouw Natural Clay Impregnation Using Titanium Dioxide as a Rhodamine B Dye Stuff Degrader. *Indonesian Journal of Chemical Research*, *9*(3), 144–149.

Bijang, C. M., Hasanela, N., Joris, S. N., Fransina, E. G., Tahril, Azis, T., & Tehuayo, A. (2023). Synthesis of Silver Nanoparticles using Gandaria Seeds Bioreductor. *Jurnal Akademika Kimia*, *12*(2), 142–148.

Dubey, S. P., Lahtinen, M., & Sillanpää, M. (2010). Tansy Fruit Mediated Greener Synthesis of Silver and Gold Nanoparticles. *Process Biochemistry*, *45*(7), 1065–1071.

Fatimah, I., & Aftrid, Z. H. V. I. (2019). Characteristics and Antibacterial Activity of Green Synthesized Silver Nanoparticles Using Red Spinach (amaranthus Tricolor L.) Leaf Extract. *Green Chemistry Letters And Reviews*, *12*(1), 25–30.

Handayani, V., Ahmad, A. R., & Sudir, M. (2014). Uji Aktivitas Antioksidan Ekstrak Metanol Bunga dan Daun Patikala (Etlingera elatior (Jack) R.M.Sm) Menggunakan Metode DPPH. *Pharm Sci Res*, *1*(1), 86–93.

Jamaludin, A., & Faizal, C. K. M. (2017). Autoclave-Assisted Synthesis of Silver Nanoparticles using Metroxylon Sagu for Antibacterial Application. *Indian Journal of Science and Technology*, *10*(6), 1–5.

Jenkins, R. (2006). X-ray Techniques: Overview. *Encyclopedia of Analytical Chemistry*, 1–20.

Lolaen, L. A. C., Fatimawali, & Citraningtyas, G. (2013). Uji Aktivitas Antioksidan Kandungan Fitokimia Jus Buah Gandaria (bouea Macrophylla Griffith). *Pharmacon Jurnal Ilmiah Farmasi*, *2*(2), 2302–2493.

Londo, N., Johannes, E., Natsir, H., & Suhadiyah, S. (2015). *Bioaktifvtas Ekstrak Kasar Biji Gandaria Bouea Macrophylla Griff Sebagai Bahan Antioksidan*. 1–8.

Nyoman Wendri, Ni Nyoman Rupiasih, & Made Sumadiyasa. (2017). Biosintesis Nanopartikel Perak Menggunakanekstrak Daun Sambiloto: Optimasi Proses Dankarakterisasi. *Jurnal Sains Materi Indonesia*, *18*(4), 162–167.

Prasetiowati, A. L., Prasetya, A. T., & Wardani, S. (2018). Sintesis Nanopartikel Perak dengan Bioreduktor Ekstrak Daun Belimbing Wuluh (Averrhoa Bilimbi L.) sebagai Antibakteri. *Indonesian Journal of Chemical Science*, *7*(2), 161–166.

Irwan, R., Teheni, M. T., & Syafriah, W. (2023). Synthesis and Characterization of Silver Nanoparticles from the Leaf Stalk Extract of Moringa oleifera. *Indonesian Journal of Chemical Research*, *11*(1), 37–42.

Rahmayani, Y., Zulhadjri, & Arief, S. (2019). Synthesis and Characterization Silver–Tricalcium Phosphate (TCP) Nanoparticle using Avocado Leaf Extract (Percea americana). *Jurnal Kimia Valensi*, *5*(1), 72–78.

Rajan, N. S., & Bhat, R. (2017). Volatile Constituents of Unripe and Ripe Kundang Fruits (Bouea Macrophylla Griffith). *International Journal of Food Properties*, *20*(8), 1751–1760.

Salasa, D., Aritonang, H., & Kamu, V. S. (2016). Sintesis Nanopartikel Perak (Ag) dengan Reduktor Natrium Borohidrida ($NaBH_4$) Menggunakan Matriks Nata-De-Coco. *Chem. Prog.*, *9*(2), 34–40.

Sari, P. I., Firdaus, M. L., & Elvia, R. (2017). Pembuatan Nanopartikel Perak (NPP) Dengan Bioreduktor Ekstrak Buah Muntingia Calabura L Untuk Analisis Logam Merkuri. *Alotrop Jurnal Pendidikan dan Ilmu Kimia.*, *1*(1), 2–26.

Shameli, K., Ahmad, M. B., Yunus, W. M. Z. W., Rustaiyan, A., Ibrahim, N. A., Zargar, M., & Abdollahi, Y. (2010). Green Synthesis of Silver/Montmorillonite/Chitosan Bionanocomposites Using the Uv Irradiation Method and Evaluation of Antibacterial Activity. *International Journal of Nanomedicine*, *5*, 875–887.

Wang, Y., Tang, W., & Zhang, L. (2015). Crystalline Size Effects on Texture Coefficient, Electrical and Optical Properties of Sputter-deposited Ga-doped ZnO Thin Films. *Journal of Materials Science & Technology*, *31*(2), 175–181.

Sari, T. I. W., Muhsin, M., & Wijayanti, H. (2018). Pengaruh Metode Aktivasi Pada Kemampuan Kaolin Sebagai Adsorben Besi (fe) Air Sumur Garuda. *Konversi*, *5*(2), 60–65.